2011 International Workshop on ADC Modelling, Testing and Data Converter Analysis and Design and IEEE 2011 ADC Forum
June 30 - July 1, 2011. Orvieto, Italy

Virtual instrument for air-coupled ultrasound NDT application based on Psuedo-Noise sequences.

Marco Ricci, Luca Senni and Pietro Burrascano

Polo Scientifico Didattico di Terni, University of Perugia, 05100 Terni, Italy

Abstract A Virtual-Instrument for Air-Coupled Ultrasound Non Destructive Testing applications based on Psuedo-Noise Sequences is presented. The instrument is designed by means of the LabView software to manage and synchronise a digital input/output module and a virtual oscilloscope and to implement the digital processing required to fully exploit the characteristics of the coded excitation. The Signal to Noise Ratio enhancement assured by this technique with respect both Additive White Gaussian Noise and Quantization Noise is theoretically analysed and experimental verified.

I. INTRODUCTION

Ultrasonic testing is a popular Non Destructive Testing (NDT) technique for the investigation of solid materials such as metals, polymers, and many others [1]–[4]. Usually a coupling medium (water, gel, oil..) is required in order to optimize the transfer of the ultrasonic energy between probes and sample under test. Nevertheless the presence of a couplant hampers the realization of On-line automatic NDT applications and it may not always be suitable for particular inspection situations, e.g. for absorbing materials or where contamination or damage would result. In this framework, one of the more promising emerging technology is represented by Air-Coupled Ultrasound due to the benefits that it provides by overcoming the need to employ a matching medium. However, ultrasonic attenuation in air is much greater than in water or gel, especially at high frequencies, and the acoustic impedance of air is much lower, leading to difficulties in the case of inspection into solid samples.

To tackle these problems, techniques that allow to enhanche the Signal-To-Noise-Ratio, *SNR*, with the current air-coupled transducers are desiderable. Among them, there are been recently reported in literature several applications based on pulse-compression techniques, especially chirp excitation [5]–[7]. In such applications a coded signal, $x[n]$, with delta-like autocorrelation function, is adopted as input to a Linear Time-Invariant System $\mathcal{L}\{\}$. The system output $y[n]$ is then correlated with the input to retrieve an estimate of the system impulse response $h[n]$:

$$y[n] = \mathcal{L}\{x[n]\} = h[n] * x[n] \rightarrow \Phi_{x,y} = \Phi_{x,x} * h[n] \simeq h[n] \tag{1}$$

where $*$ denotes the convolution operator, $\Phi_{x,y}[n]$ is the cross-correlation function of x and y, and we have assumed $\Phi_{x,x}[n] \simeq \delta[n]$. In the presence of environmental noise, pulse-compression techniques allow to significantly enchance the *SNR* by injecting into the system higher energy with respect to standard impulse-response measurement schemes. Here we report the realization of a pulse-compression measurement procedure for Air-Coupled Ultrasound applications based on Pseudo-Noise excitation. In particular we adopt *m*-sequences, also known as Maximum Length Sequences or Galois Sequences [8]–[11]. The paper is organized as follows: in Section II we briefly introduce the *m*-sequences and the relative impulse response measurement procedure; in Section III we characterize this procedure in term of SNR enhancement with respect Additive White Gaussian Noise, *AWGN*, and Quantization Noise, *QN*. The adopted experimental set-up and some results are presented in Section IV while in Section V we draw some conclusions and future developments of the procedure here presented.

II. *m*-SEQUENCES: PROPERTIES AND APPLICATION

m-sequences are periodic binary codes with period length $L = 2^N - 1, N \in \mathbb{N}$ that can be generated by means of a Linear Feedback Shift Register with N delay taps. Actually each *m*-sequence, $\{m[k] : k \in [1, L], m[k] \in \{-1, 1\}\}$ is associated to a recursive equation like: $m[k+N] = \prod_{i=0}^{N-1} m[k+i]^{\alpha_i}$ where the $\alpha_i : \{0, 1\}$ are the coefficients of a primitive polynomial on the Galois field $GF(2^N)$. N is called the order of the sequence and for any order N different primitive polynomials can be adopted. Each polynomial leads to a distinct sequence. The properties of the *m*-sequences have been formulated by Golomb in [8]; the most charming ones for pulse compression applications are: (i) the cyclic autocorrelation function of an *m*-sequence is a very close approximation to a delta function: $\Phi^{cyc}_{m,m}[n] = 2^N\delta[n] - \theta[n]$, (ii) their power density spectrum is flat, with the exception of a near-zero DC term; (iii) a fast transform, the so called Fast *m*-Transform, exists to carry out correlation between *m*-sequences and output signal $y[n]$: $\Phi_{m,y}[n] = \mathcal{FMT}(y[n])$ [12]. In impulse response measurement applications, the *m*-sequences are adopted as input signal of the LTI system to be characterized. By assuming that the impulse response $h[n]$ of the system vanishes $\forall\ n \geq L$, the output is also periodic with the same period, apart a transient signal L samples length. Mathematically the output can be described by the compact espression:

$$\begin{bmatrix} \mathbf{y_{tr}} \\ \mathbf{y} \\ \vdots \\ \mathbf{y} \end{bmatrix} = \begin{bmatrix} M_{tr} \\ M_{cyc} \\ \vdots \\ M_{cyc} \end{bmatrix} \cdot \mathbf{h} \tag{2}$$

where

$$M_{tr}=\begin{bmatrix} m[0] & 0 & \cdot & 0 \\ m[1] & m[0] & \cdot & 0 \\ \cdot & \cdot & \cdot & \cdot \\ m[L-2] & m[L-3] & \cdot & 0 \\ m[L-1] & m[L-2] & \cdot & m[0] \end{bmatrix}; M_{cyc}=\begin{bmatrix} m[0] & m[L-1] & \cdot & m[1] \\ m[1] & m[0] & \cdot & m[2] \\ \cdot & \cdot & \cdot & \cdot \\ m[L-2] & m[L-3] & \cdot & m[L-1] \\ m[L-1] & m[L-2] & \cdot & m[0] \end{bmatrix} \mathbf{h}=\begin{bmatrix} ;h[0] \\ h[1] \\ \cdot \\ h[L-1] \end{bmatrix}; \mathbf{y_{tr}}=\begin{bmatrix} y_{tr}[0] \\ y_{tr}[1] \\ \cdot \\ y_{tr}[L-1] \end{bmatrix}; \mathbf{y}=\begin{bmatrix} y[0] \\ y[1] \\ \cdot \\ y[L-1] \end{bmatrix}.$$

The single output period, $\mathbf{y}$, is therefore described by the cyclic convolution of the sequence $m[n]$ with the impulse response: $\mathbf{y}=M_{cyc}\cdot\mathbf{h}$. The properties of the *m*-sequences assure that, once measured $\mathbf{y}$, the impulse response $h[n]$ can be estimated with good approximation by cross-correlating the output with the input sequence. In particular definying the time-reversed sequence $\overleftarrow{m}[n]=\{m[0],m[L-1],..,m[1],m[0],m[L-1],..\}$, the cross-correlation procedure is equivalent to convolve the system output $y[n]$ with $\overleftarrow{m}[n]$. This convolution process then assumes the matrix notation

$$h[n]\simeq\hat{h}[n]=\Phi_{y,m}[n]=\frac{1}{L}\overleftarrow{M}_{cyclic}\cdot\mathbf{y}=\frac{1}{L}\overleftarrow{M}_{cyclic}\cdot M_{cyclic}\cdot\mathbf{h}=M^{-1}_{cyclic}\cdot M_{cyclic}\cdot\mathbf{h} \text{ with } M^{-1}_{cyclic}=\frac{1}{L}\begin{bmatrix} m[0] & m[1] & \cdot & m[L-1] \\ m[L-1] & m[0] & \cdot & m[L-2] \\ \cdot & \cdot & \cdot & \cdot \\ m[2] & m[3] & \cdot & m[1] \\ m[1] & m[2] & \cdot & m[0] \end{bmatrix} \quad (3)$$

It was found that the reverse sequence $\overleftarrow{m}[n]$ is also an *m*-sequence corresponding to a different primitive polinomial and that $\overleftarrow{M}_{cyclic}=(M_{cyclic})^T$ [13]. The δ-like autocorrelation property of the *m*-sequences can be re-expressed in matrix form by the relation $M^{-1}_{cyclic}\cdot M_{cyclic}=\frac{1}{L}\overleftarrow{M}_{cyclic}\cdot M_{cyclic}=\frac{L+1}{L}\mathcal{I}_{L,L}-\frac{1}{L}ones(L,L)$ that implies:

$$\hat{h}[n]=\frac{L+1}{L}h[n]-\frac{\sum_{n=1}^{L}h[n]}{L}=\frac{L+1}{L}h[n]-mean(h[n]) \quad (4)$$

For zeromean AC signals, like those produced by ultrasound probes, $\hat{h}[n]$ coincides with $h[n]$ unless for a multiplicative factor approaching the unit value for large L. Henceforth we only consider AC signals. By contextually assuring a costant delivered power over a long excitation time and maintaining the spectral power characteristic of an impulsive excitation, the *m*-sequences Impulse Response Measurement (*mIRM*) scheme above described thus exhibits the typical feature of pulse-compression techniques. As further feature of the procedure that is of useful in real applications, the cross-correlation step needed to retrieve the system impulse response, i.e. the matrix multiplication $\overleftarrow{M}_{cyclic}\cdot\mathbf{y}$, can be implemented by adopting the Fast *m*-Transform, that requires $\mathcal{O}(L\ lnL)$ addictions and subtractions [12]. In real applications the measured data are affected by environmental noise and in this case the properties of the *m*-sequences measurement protocol allow to estimate the impulse response $h[n]$ even in the presence of a high noise power and/or by using excitation signals at a very low power level [14]. Due to the large diffusion of Digital Signal Processing and digital electronic components, actual applications always include a quantization process where the noisy output signal is digitalized. The *mIRM* method is well known for the *SNR* enhancement it assure with respect to additive noise, and it has found a widespread application especially in acoustics where it has become a standard. However an analysis of its performance with respect to quantization process has not been reported in the literature. In the next section we briefly recall how the *AWGN* is attenuated by adopting such scheme. Furthermore we enlight some features of the procedure that also lead to a reduction of the quantization noise, strengthen the efficacy and the robustness of the protocol.

III. *m*-SEQUENCES: SNR IMPROVEMENT

In real applications, the *mIRM* method can be summarized by Fig.1 (a) where both the environmental and the quantization noise have been introduced. The whole process described by Eq.3 can be viewed as a *transform coding* scheme developed to optimally transmit the impulse response $h[n]$ over the quantization channel $\mathcal{Q}$. In this perspective $\hat{h}[n]$ represents the received signal and the pair of matrices $M_{cyclic},\overleftarrow{M}_{cyclic}$ acts like pre- and post-filters respectively. and both the AWGN and the QN can be reduced.

A. *SNR enhancement with respect to AWGN*

The energy content of the exciting signal corresponding to the use of ideal *m*-sequences is $E=\left(2^N-1\right)V_{cc}^2$, where the sequence values $\{+1,-1\}$ have been associated to the voltage values $\{+V_{cc},-V_{cc}\}$ respectively. If compared with the energy content of a single pulse of the same amplitude V_{cc}, the *mIRM* scheme ensures a SNR enhancement $G_{AWGN}\simeq 10\log_{10}\left(2^N\right)\simeq 3*N[db]$. Typical sequence orders adopted in the experiments reported in this paper range from $N=14$ to $N=18$ assuring a gain ranging respectively from $G_{AWGN}=32[db]$ to $G_{AWGN}=48[db]$. This SNR gain can be derived also by exploiting Eq.4, i.e. after pulse compression. Suppose that the measured data are affected by AWGN $e[n]$ with standard deviation σ_{AWGN}:$y[n]=M_{cyclic}\cdot\mathbf{h}+e[n]$, corresponding to a SNR equal to C. What is the resultant noise on the estimated impulse response? From Eq.4 it follows that in this case we have: $\hat{h}[n]=\frac{L+1}{L}h[n]+\tilde{e}[n]$, where $\tilde{\mathbf{e}}=M^{-1}_{cyclic}\cdot\mathbf{e}$ is the noise after the cross-correlation step. Since all the elements of the $\overleftarrow{M}_{cyclic}$ are -1's and 1's, and being the values of $\tilde{e}[n]$ at different n values uncorrelated, it is a straightforward consequence of the *Bienaymé* formula that the standard deviation $\tilde{\sigma}$ of $\tilde{e}[n]$ is

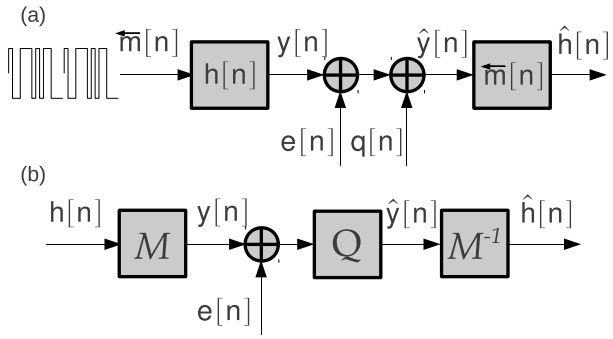

Fig. 1. Block diagram of the *m*-sequences impulse response measurement scheme.(a) circuit representation in terms of convolution: the input sequence $m[n]$ excite a LTI system characterized by an impulse response $h[n]$. The resulting output signal $y[n] = (m[n] * h[n])_{cyclic}$ is then affected by both environmental additive noise $e[n]$ and by quantization noise $q[n]$. The estimated impulse response $\hat{h}[n]$ is attained by convolving the noisy output signal $\hat{y}[n] = y[n] + e[n] + q[n]$ with the time-reversed input sequences $\hat{h}[n] = (\overline{m}[n] * \hat{y}[n])_{cyclic}$ (b) transform coding representation: the matrices M_{cyclic} and $(M_{cyclic})^T$ corrispond to the pre and post filter blocks interleaved by the quantization channel $\mathcal{Q}$.

equal to: $\tilde{\sigma} = \frac{\sigma}{\sqrt{L}} \simeq \frac{\sigma}{2^{\frac{N}{2}}}$ [15]. Moreover the resulting error is AWGN too, according with the *Central Limit Theorem* (*CLT*). By increasing the order N, i.e. the sequence length, the noise power decreases monotonically leading to a SNR enhancement $G_{AWGN} \simeq 3 * N[db]$, as expected.

B. SNR enhancement with respect to QN

Quantization is a lossy process in wich a signal $x[n]$ is quantizated to one of 2^B discrete levels where B is the number of binary digits used to represent each sample. The quantizated value of the sample $x[n]$ is denoted by $\hat{x}[n]$ and is related to $x[n]$ by : $\hat{x}[n] = x[n] + q[n]$ where $q[n]$ is an additive noise term or error introduced by the quantization process. The theme of optimising the overall coding system in order to improve the performance of a simple uniform quantiser has been deeply discussed in the last decades. One of the most important schemes adopted to approaches the problem of optimising the performance of a quantiser relies on pre- and post- filters around the quantiser. Different implementations of this scheme lead, for instance, to the Differential PCM System [16], of which the Delta Modulation Systems can be considered as a sub class. In [17] the case where the quantisation system is a simple quantiser and the postfilter is constrained to be the inverse of the prefilter was analysed. [17] shows that the magnitude response of the optimum pre and post filter must follow the so called "half whitening" scheme. If the filtering and quantization system is split in the parallel of M different channels, we have a Sub-Band Coding System [18], in which the allocation of the B available bits among the different sub-bands, together with the optimization of pre and post filters, is a relevant part of the optimization process. Transform Coding (or Block Quantization) makes a different use of the linear dipendencies among samples based on a "frequency domain" approach, where the order of the transform (i.e. the number of transform coefficients) assumes a role similar to sub bands [19]. Although *mIRM* does not belong in one of these techniques, it resembles the Transform Coding approach (see Eq.3 and Fig.1-b) and we found that it is robust with respect to QN, allowing to reduce it by combining different advantageous effects, as explained in the following. To quantify these benefits it is convenient to introduce a measure of the efficiency of the source coding technique provided by the ratio of signal to quantization noise power, here denoted by SNR_{QN}. Mathematically, SNR_{QN} is defined by : $SNR_{QN} = 10 \log \frac{\mathcal{E}(x^2[n])}{\mathcal{E}(q^2[n])}$. It was found that the amount of QN power and its statistical properties are related both to the statistical properties of the signal $x[n]$ and to the number of bits of the digitizer. In the general case, i.e. for a sufficient high value of B, the original signal is much larger than the quantization step Δ. When this happens, the quantization error $q[n]$ can be assumed to be not correlated with the signal, and described by a uniform probability density function: $p(q[n]) = \begin{cases} \Delta^{-1}, & \text{if } -\frac{\Delta}{2} \leq q[n] \leq \frac{\Delta}{2} \\ 0, & \text{otherwise} \end{cases}$ With this assumption we have $\mathcal{E}(q^2[n]) = \frac{\Delta^2}{12}$. Now consider the scheme of Fig.1-a, where the QN is regarded as a second additive noise source with uniform PDF. By applying also in this case the *Bienaymé* formula and the *CLT*, we have that the variance of the quantization noise σ_{QN} after the cross-correlation step is reduced by a factor $\sqrt{L} = 2^{\frac{N}{2}}$ and that the trasformed noise sequence $\hat{q}[n]$ exhibits a gaussian PDF. Actually the same SNR gain, $3N[db]$ is achieved indipendently for AWGN and QN noises. In the most general case, where they are simoultaneously present, this factor holds with respect to the overall noise power, given by $\mathcal{E}\big((e[n]+q[n])^2\big)$. If the $e[n]$ and $q[n]$ are assumed to be uncorrelated and with zero-mean, then $\mathcal{E}\big((e[n]+q[n])^2\big) = \mathcal{E}\big(e[n]^2\big) + \mathcal{E}\big(q[n]^2\big)$. This is the first benefit of the *mIRM* procedure with respect to QN. Another positive effect consists of the reduction of the peak factor P of the convolved signal $y[n]$ compared with the one of the signal to be estimated, $h[n]$. The peak factor P (or crest factor) is a measure of the height of the peak value of a signal in relation to the amount of power carried by the signal. It is defined as the ratio of the peak-to-peak signal amplitude,

x_{pp}, to the root mean square value of $x[n]$: $P = \frac{x_{pp}}{\sigma_x}$. The square wave takes on the lowest among the possible values of the peak factor: in fact in this case $\frac{V_{pp}}{\sigma} = 2$, while for a sine wave it takes on a value of $2\sqrt{2}$. It can be seen that the QN power dependes quadratically from the peak factor of the signal to be quantizated, say $x[n]$. Indeed, by assuming that the amplitude range of $x[n]$ is represented by R_x, for a B-bits uniform digitizer, the step size Δ can be expressed as $\Delta = \frac{x_{pp}}{2^B}$ and SNR_{QN} turns out to be:

$$SNR_{QN} \simeq 6B + 10.8 + 10log\frac{\mathcal{E}(x^2[n])}{x_{pp}^2} = 6B + 10.8 + 20log\frac{\sigma_x}{x_{pp}} = 6B + 10.8 - 20log(P)[db] \quad (5)$$

Lowering P then leads to a significant reduction of the QN even before applying pulse compression. In literature have been reported several strategies to attain periodic signals of a specified power spectrum having a low or minimum peak factor P [20]–[25]. Such signals are desirable in many applications like radar, sonar, communication techniques, speech synthesis, and the design of test signals for parameter estimation purposes. In the majority of these and other applications, the purpose of minimizing the peak factor is simply to maximize the signal power within the allowable amplitude range. For a specified power spectrum, the peak factor of a periodic signal is a function of the phase angles of the harmonics: if the orignal signal is $x[n] = \sum_{k=M1}^{M2} \alpha_k \cos(k\omega_0 t + \phi_k)$, proper phase angles are added to the different harmonics to provide a new signal $\tilde{x}[n] = \sum_{k=M1}^{M2} \alpha_k \cos(k\omega_0 t + \phi_k + \delta\phi_k)$ with the same power spectrum of $x[n]$ but with a smaller P. Among the possible strategies to be pursued to accomplish this aim, Schroeder [20] proposed two optimal solutions: one that consider continous values of $\{\delta\phi_k\}$ derived by a simple, intuitive rule based on an asymptotic relationship between the power spectra of frequency-modulated signals and their instantaneous frequencies; the other limits the $\{\delta\phi_k\}$ values to be 0 or π. It can be seen that the present scheme represents an intermediate situation in which the phases $\{\delta\phi_k\}$ assume a finite set of value, precisely all the L complex roots of the unit. In the numerical experiments here not reported, we found that the peak factor reductions attained with this protocol are also intermediate between the maximum ones attained by the *continous angle* strategy and the ones achievable by adotping the *discrete angle* strategy. In this case the role of $x[n]$ is held by $h[n]$, while $\tilde{x}[n] \rightarrow y[n]$. To apply the Schroeder formula we have exploited the matrix identity

$$\begin{bmatrix} M_{tr} \\ M_{cyc} \\ \vdots \\ M_{cyc} \end{bmatrix} \cdot \mathbf{h} = \begin{bmatrix} H_{tr} \\ H_{cyc} \\ \vdots \\ H_{cyc} \end{bmatrix} \cdot \mathbf{m} = \begin{bmatrix} \mathbf{y_{tr}} \\ \mathbf{y} \\ \vdots \\ \mathbf{y} \end{bmatrix}; H_{tr} = \begin{bmatrix} h[0] & 0 & \cdot & 0 \\ h[1] & h[0] & \cdot & 0 \\ \cdot & \cdot & \cdot & \cdot \\ h[L-2] & h[L-3] & \cdot & 0 \\ h[L-1] & h[L-2] & \cdot & h[0] \end{bmatrix}; H_{cyc} = \begin{bmatrix} h[0] & h[L-1] & \cdot & h[1] \\ h[1] & h[0] & \cdot & h[2] \\ \cdot & \cdot & \cdot & \cdot \\ h[L-2] & h[L-3] & \cdot & h[L-1] \\ h[L-1] & h[L-2] & \cdot & h[0] \end{bmatrix}$$

meaning that the periodic output signal is mathematically equivalent to the convolution of a periodic repetition of the impulse response to be measured, $h_{periodic}$, with a sigle period of the *m*-sequence. Actually the *m*-sequence acts as like an all-pass filter (execpt the DC frequency that vanishes in the systems we want to characterized) that introduce a different phase-delay for each harmonic that constitue the periodic sequence $h_{periodic}$. For typical ultrasound signals we are dealing with, the reduction of P can be as high as 10, leading to a SNR_{QN} gain up to $20[db]$ before pulse compression. The combination of the two effects previously described allows to significantly attenuate the influence of the QN on the retrieved impulse response. Moreover from Eq.3 we note that $\hat{h}[n]$ has nearly the same amplitude of $h[n]$ but it is discretised in levels 2^N times smaller then $h[n]$, thus appearing to come out from a quantiser with $B' = B + N$ bits. Some experimental results showing these aspects are reported in the next Section. At low values of B, or equivalently at low signal levels, the quantization error becomes dependent on the input signal, resulting in distortion. In this case the modelization of the QN as an additive noise source does not hold yet. In order to make the quantization error independent of the input signal, noise with an amplitude of 2 least significant bits is added to the signal. This slightly reduces signal to noise ratio, but, ideally, completely eliminates the distortion. It is known as dither. In our case, for very low signals we usually have $|e[n]| > |y[n]|$, then the QN is correlated with the AWGN instead of with the true signal. An analytical treatment of this case lies outside the scope of this work; we limited to report some experimental results attained by gradually incresing the QN up to a level that completely cancel the SNR gain introduced by the *mIRM* scheme.

IV. EXPERIMENTAL SET-UP

The experimental set-up adopted to test the *m*-sequence impulse response measurement scheme for air-coupled ultrasound is depicted in Fig.1. Since standard NDT ultrasound hardwares do not exhibit the flexibility in signal generation, acquisition and processing needed to fully implement the procedure, we have developed a Virtual Instrument by means of the LabView Software that allows to: (i) generate a coded signal able to drive a suitable ultrasound pulser by means of a Digital Input Output (DIO) module NI-PXI 6534 operating up to 20 MHz; (ii) guarantee the synchronization between the excitation signal and the digitalization of the receiving probe signal carried out by employing a 12-bit Digital Oscilloscope Module NI PXI-5105 with maximum sample rate of 60MS/s and with 60 MHz of bandwidth; (iii) perform in real-time the processing of the measured data through the application of the Fast *m*-Transform; (iv) visualize simultaneously the acquired data $y[n]$, the reconstructed impulse response $h[n]$,its envelope and its $\mathcal{FFT}$ amplitude.. Typical values of the parameters adopted in the experiments reported below are: probe center frequency $f_0 = 200kHz$, $V_{cc} = 40[V]$, *m*-sequence generation rate $f_m = 400KS/s$, acquisition rate

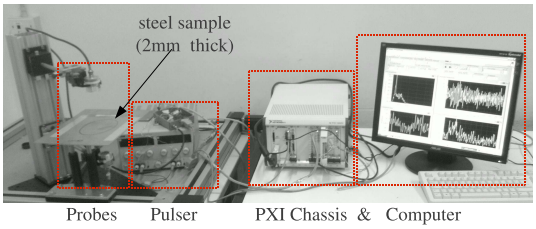

Fig. 2. Experimental Set-Up Adopted: A computer embedded in a National PXI Chassis manages the data processing as well as the hardware signal generation and acquisition tasks by means of the LabView software; the output signal drives an Ultrasound Pulser operating between $\pm V_{cc}$ with $0 < V_{cc} < 60[V]$; the pulser excites the transmitter probe while the output signal of the receiving probe is directly digitalized by the NI-Scope Module. There are also shown: (I) a pair of point-focused probes from ULTRAN operating at 200 kHz and arranged in transmission configuration and (II) one of the sample tested, a $2mm$ thick plate of stainless steel.

$f_s = 6MS/s$. Moreover a Butterworth digital filter can be applied to the measured data before the cross-correlation step. Nevertheless in the experiments here reported the filter was disabled to fair asses the SNR gain provided by the only adoption of *m*-sequences excitation. In Figures 2 and 3 the Front Panel and Block Diagram of the VI are reported respectively. The

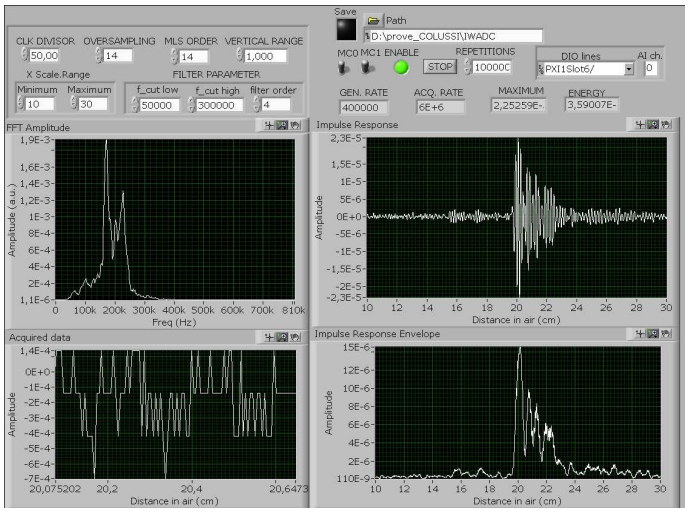

Fig. 3. Front Panel of the Virtual Instruments developed: in the top left corner are arranged all the controls regarding the generation and acquisition tasks: Clock divisor for the DIO module, oversampling factor for the Scope module respect the generation rate, vertical range, *m*-sequence order N, range of visualization (in cm @ air sound velocity) and the parameters of a Butterworth pass-band digital filter optionally applyed to the acquired data. In the top right corner are instead displaced the controls relating the files and the hardware managment. There are also shown some indicators that allow to check the rigth working of the system. The bottom side of the panel is subdivided in four subplot showing respectively the amplitude spectrum of $h[n]$, the impulse response $h[n]$, the acquired data and the full-wave envelope of $h[n]$.

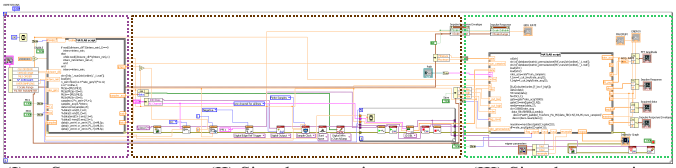

Fig. 4. Block Diagram of the Virtual Instruments developed where have been evidenced three main steps of the procedure: (I) the numerical generation of the selected *m*-sequence $m[n]$; (II) the synchronous generation and acquisition of $m[n]$ and of the system output signal $y[n]$; (III) the data processing and the subsequent results visualization.

experiments have been carried out in *through-transmission* configuration; in order to verify the SNR improvement assured by *mIRM* we have compared the retrieved impulse response in air with the one attained by introducing an aluminum, *Al*, plate 3mm thick between the two probes (see Fig.2). In this configuration the attenuation of the ultrasonic energy is about $80[db]$ due to the high mismatching of the acoustic impedance of air and *Al* that introduce a signal attenuation of $40[db]$ at any

air-*Al* interface. The measured impulse response in air exhibits a peak value of few tens of *mV*, therefore after the insertion of the Al*Al* plate we expected an impulse response amplitude of few μV, lower than the minimum ADC quantization step $\Delta_{min} =\simeq 14\mu V$. Nevertheless for sufficient high N the reconstructed impulse response $h[n]$ is well defined in term of both SNR and bit-resolution. To quantitative estimate the SNR gain provided by the *mIRM* method we have carried out a set of measurements by varying: (a) the sequence order N, (b) the V_{cc} value and (c) the vertical input range of the digitizer to vary the quantization step Δ. Some results of these experiments are reported in Fig.5 where the impulse response in air is compared with the impulse response in presence of the *Al* plate for different N and V_{cc} values. The SNR enhancement is in agreement with that illustrated in Section III assured by the properties of *m*-sequences;. Of course the SNR gain increases linearly with respect to V_{cc} too. In particular an enhancement of a factor 2 of V_{cc} increase the SNR of about $6[db]$. The SNR dependance from V_{cc} allows to better asses the benefit of the procedure, indeed by analyzing Fig.5 it can be seen that the SNR is approximately the same for the signals reported in subplots 2 and 9, corresponding to $\{N = 14, V_{cc} = 40[V]\}$ and $\{N = 16, V_{cc} = 20[V]\}$, as expected. Moreover the minimum value of the SNR necessary to faithfully discriminate the impulse response from the noise, is attained for $\{N = 16, V_{cc} = 5[V]\}$ corresponding to $\{N = 10, V_{cc} = 40[V]\}$ from which we estimate a limit value of SNR gain necessary to measure the wanted impulse response equal to $30[db]$.

For the sake of completeness, also a comparison with the standard *'single pulse'* measurement has been carried out. In particular we have compared the impulse response attained by adopting: (a) a $N = 18$ *m*-sequence with $V_{cc} = 40[V]$, (b) a train of ≈ 1200 identical single pulses of the same amplitude $V_{cc} = 40[V]$, delayed of $300mm@air$, corresponding to the minimum distance necessary to cover all the impulse response. This pulse train has a time duration that equals the $N = 18$ sequence, thus the comparison has been carried out with the same peak power and with the same time of excitation. The response to that train has been averaged over all the pulses to optimized the SNR ratio (Fig6-b). The average precedure assures a SNR gain equal to $G_{SNR}^{average} = 10log(N_{average})$ with $G_{SNR}^{average} \approx 31[db]$ in this case comparable with the one of Fig.5-subplot6 that is not sufficient high to allow discrimination of the impulse respone $h[n]$. Then for the present configuration, i.e. impulse response duation, the *mIRM* method assures a significantly better performance then the average stretegy. In general, longer is the impulse response to be measured, higher is the gain provided by the *mIRM* scheme as well known. As

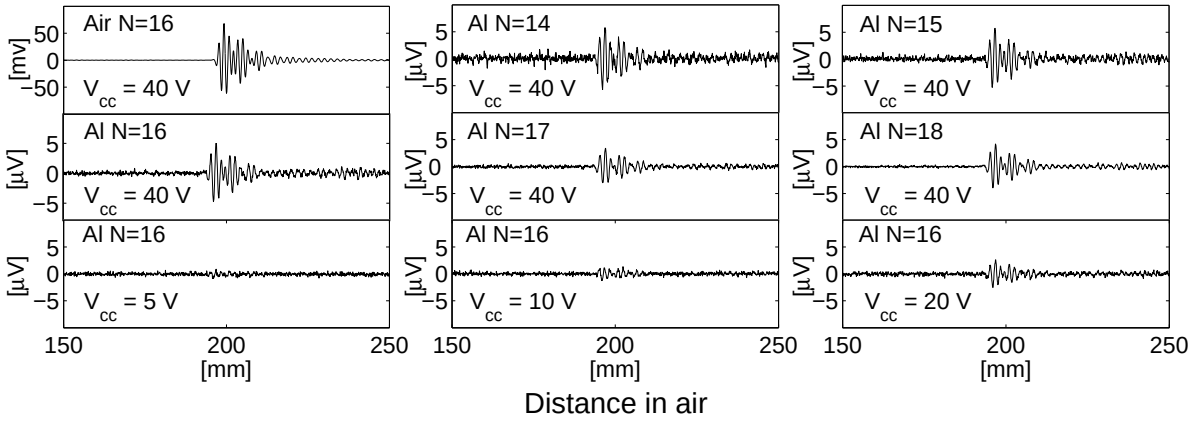

Fig. 5. Acquired data and corresponding reconstructed impulse response for different *m*-sequences order N and V_{cc} values. The monothonic enhancement of the SNR with N is clearly evident.

further analysis, in Fig. 7 are reported three measurements carried out with $N = 16$ and $V_{cc} = 40[V]$ by varying the ADC input range to increase the quantization step Δ and consequently the QN power. Precisely we have acquired data with three different quantization levels corresponding respectively to $\Delta = 14, 278, 1700[\mu V]$. Actually with respect to the lower resolution ($\Delta = 14[\mu V]$), for $\Delta = 278, 1700[\mu V]$ we artificially introduce a SNR attenuation of ≈ 25 and $40[db]$ respectively. For the first case, $\Delta = 278[\mu V]$, the SNR gain provided by the pulse-compression procedure $G_{SNR} \approx 3 * N = 48$ is yet sufficient high to retrieve with acceptable noise level the wanted impulse response even in presence of *Al*, while for the second case the SNR attenuation completely counterbalance the *mIRM* SNR enhancement. These results are in agreement with ones reported in Figures 5 and 6.

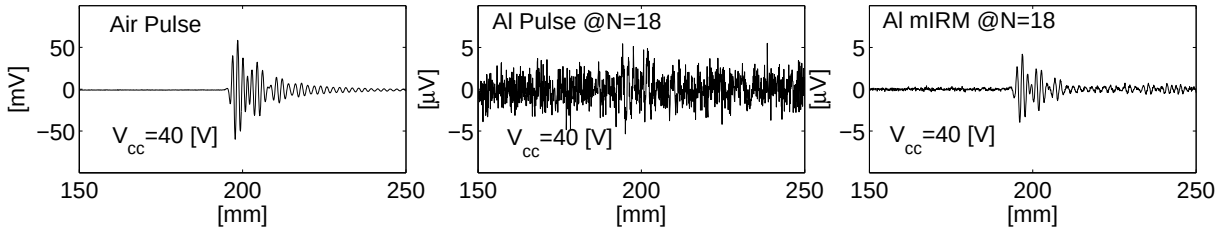

Fig. 6. (a) single pulse in air, (b)averaged single pulse with *Al* plate, (c) *mIRM* result with *Al* plate

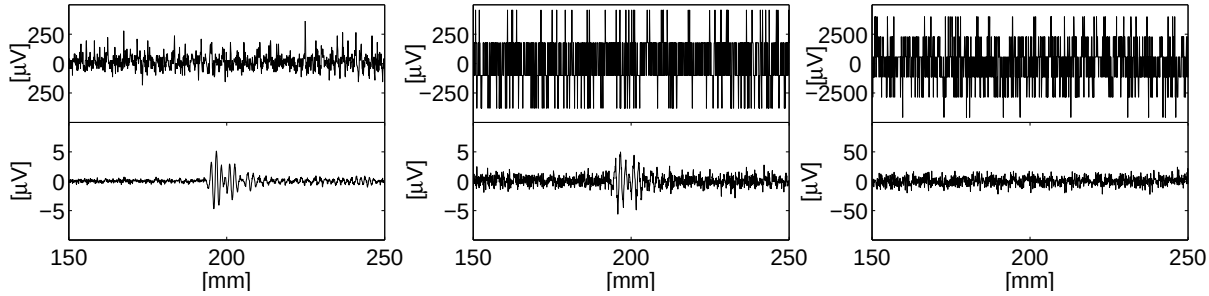

Fig. 7. Reconstructed impulse responses by adopting a *sequences* of order $N = 16$, $V_{cc} = 40[V]$ and by varing the quantization step: (a) $\Delta = 14[\mu V]$, (b) $\Delta = 278[\mu V]$ and (c) $\Delta = 1700[\mu V]$.

V. CONCLUSIONS AND PERSPECTIVES

We have reported the application of the *m*-sequence impulse response measurement scheme in air-coupled ultrasonic NDT. In particular we have analysed the SNR gain provided by this method with respect both additive environmental and quantization noise. We have showed by theoretical arguments and demonstrated by experimental measurements the effectiveness of the procedure even in presence of hard conditions like high attenuating media, low bit quantizer and poor channel SNR. A more detailed analysis of the performance of the *mIRM* scheme for coulored additive noise as well as for low bit number quantiser should be undertaken in a future work.

ACKNOLEDGEMENTS

The authors acknowledge financial support from the *Fondazionde Cassa di Risparmio di Terni e Narni*

REFERENCES

[1] L. W. Schmerr, *Fundamentals of ultrasonic nondestructive evaluation: a modeling approach*, Springer, Berlin (1998).
[2] J.L. Rose, *Ultrasonic Waves in Solid Media*, Cambridge University Press, Cambridge, (2004).
[3] J.Blitz, G. Simpson, *Ultrasonic Methods of Non-destructive Testing* in Non-Destructive Evaluation Series, Vol. 2, Springer, Berlin, (1995).
[4] I.N. Prassianakis and N.I. Prassianakis, Ultrasonic testing of non-metallic materials: concrete and marble, *Theoretical and Applied Fracture Mechanics* **42**, (2), 191-198 (2004).
[5] T.H. Gan, D.A. Hutchins, D.R. Billsona and D.W. Schindelb, The use of broadband acoustic transducers and pulse-compression techniques for air-coupled ultrasonic imaging , *Ultrasonics*, **39**, (3), 181-194 (2001).
[6] P. Pallav, T.H. Gan, D.A.Hutchins, Elliptical-Tukey chirp signal for high-resolution, air-coupled ultrasonic imaging. *IEEE Trans Ultrason Ferroelectr Freq Control* **54**,(8), 1530-40 (2007).
[7] M.Garcia-Rodriguez, *et. al*, Application of Golay codes to improve the dynamic range in ultrasonic Lamb waves air-coupled systems, *NDT & E International* **43**,(8), 677-686 (2010).
[8] S. Golomb, *Shift Register Sequences*, San Francisco, Holden–Day, (1967).
[9] D.V. Sarwate, M.B. Pursley, Crosscorrelation properties of pseudorandom and related sequences, *Proceedings of the IEEE* **68**, (5), 593 - 619 (1980).
[10] M. R. Schroeder, *J. Acoust. Soc. Am. 66*, 497–500 (1979).
[11] P. Burrascano, M. Carpentieri, A. Pirani, M. Ricci, Galois sequences in the non-destructive evaluation of metallic materials, *Measurement Science &Technology* **17**, (11), 2973-2979 (2007).
[12] M. Cohn and A. Lempel, On Fast M-Sequence Transforms, *IEEE Trans. Information Theory* **IT-23**, 135–137, (1977).
[13] N. Xiang, M.R. Schroeder, Reciprocal maximum-length sequence pairs for acoustical dual source measurements *J. Acoust. Soc. Am.* **113** (5), 2754-2761 (2003).
[14] M. R. Schroeder, Integrated-impulse method measuring sound decay without using impulses *J. Acoust. Soc. Am.* **66**, (2), 497-500 (1979).
[15] M. Loeve, *Probability Theory*, Volume 45, 4^{th} ed., Springer-Verlag, (1977).
[16] C.C. Cutler, *Differential Quantization for Communication Signals*, U.S. Patent 2.605.361, July 29, (1952).
[17] N.S. Jayant, P. Noll, *Digital coding of waveforms: Principles and applications to speech and video*, Prentice-Hall, Englewood Cliffs, N.J., (1984).

[18] J. Tuqan, P.P. Vaidyanathan, Statistically optimum pre- and postfiltering in quantization, *IEEE Trans. on Circuits and Systems II: Analog and Digital Signal Processing*, **44**, (12), 1015 - 1031 (1997).
[19] N. Ahmed, K.R. Rao, *Orthogonal transforms for Digital Signal Processing*, Springer-Verlag, New York, (1975).
[20] M. R. Schroeder, Synthesis of low-peak-factor signals and binary sequences with low autocorrelation, *IEEE Trans. Inform. Theory*, **IT-16**, 85–89 (1970).
[21] S. Boyd, Multitone signals with low crest factor, *IEEE Trans. Circuits Syst.*,**CAS-33**, 1018–1022 (1986).
[22] A. van den Bos, A new method for synthesis of low-peak-factor signals, *IEEE Trans. Acoust., Speech, Signal Processing*, **ASSP-35**, 120–122 (1987). A. Horner and J. Beauchamp: GA-optimized peak factors, J. Acoust. Soc. Am. 99 (1), (1996).
[23] E. van der Ouderaa, J. Schoukens, and J. Renneboog, Peak factor minimization using a time-frequency domain sapping algorithm, *IEEE Trans. Instrum. Meas.* **38**, 145–147 (1988).
[24] A. Potchinkov, Low-crest-factor multitone test signals for audio testing, *J. Audio Eng. Soc.* **50**, (9), 681–694 (2002).
[25] Hayashi, T. Okawa, S. Low-Peak Pseudo-White-Noise Arrays, *IEEE Signal Processing Letters* **11**, (2), (2004).